

## Mesoscale reverse stick-slip nanofriction behavior of vertically aligned multiwalled carbon nanotube superlattices

J. Lou,<sup>a)</sup> F. Ding, H. Lu, J. Goldman, Y. Sun, and B. I. Yakobson

*Department of Mechanical Engineering and Materials Science, Rice University, Houston, Texas 77005, USA*

(Received 16 March 2008; accepted 5 May 2008; published online 23 May 2008)

Characteristics of sliding friction behaviors of vertically aligned multiwalled carbon nanotube (CNT) superlattices have been investigated in this letter. Friction force was measured using both regular atomic force microscopy (AFM) probe and colloidal AFM probe consisting of a 15  $\mu\text{m}$  diameter borosilicate sphere attached to the end of regular cantilever. A distinct reverse stick-slip behavior was observed in the current study compared to the usual stick-slip behavior reported in literature. It was found that this reverse stick-slip behavior was primarily due to the combined effects of surface topology and elastic deformation of CNTs, which were verified by experiments and atomistic simulations. © 2008 American Institute of Physics. [DOI: 10.1063/1.2936866]

The understanding and control of frictional behaviors of matter at the nanometer length scale is of critical importance to both to reveal the underlying physical mechanism behind friction, and to advance many nanotechnology innovations ranging from nanorobotic manipulations<sup>1</sup> to microelectromechanical system (MEMS)/nanoelectromechanical system (NEMS) with sliding interfaces.<sup>2–4</sup> Using a friction force microscope, Mate *et al.*<sup>5</sup> reported the first atomic friction study of a tungsten tip sliding over graphite, and observed a sawtoothlike modulation of the lateral force with sliding distance due to the gradual-stick and subsequent rapid slip of the tip (the usual “stick-slip” motion) with periodicities corresponding to the graphite’s honeycomb structures. The atomic stick-slip behavior was found in many friction experiments performed at the nanometer length scale by atomic force microscopy<sup>5–7</sup> (AFM) and was thought to be closely related to the fundamental energy dissipation mechanisms of friction.<sup>3,4,8,9</sup> Understanding this elastic instability caused by interactions between the cantilever lateral stiffness, elastic contact stiffness, and the corrugation of the periodic interfacial potentials,<sup>3,8</sup> may provide insights into the origins of friction and lead to better strategies for controlling it. Meanwhile, carbon nanotubes (CNTs) have been explored as promising alternatives for many tribological applications due to the predicted weak intermolecular bonding of CNTs with countersurfaces.<sup>10</sup> Friction behavior of vertically and transversely aligned CNT forests<sup>11–13</sup> and superlattices<sup>14,15</sup> at the micron and nanometer length scales were investigated due to their promising potentials in MEMS/NEMS applications.

Highly ordered arrays of multiwalled CNTs embedded in a hexagonal close-packed alumina template were grown by a chemical vapor deposition technique.<sup>15,16</sup> The vertically aligned multiwalled CNTs (VAMWCNTs) were then partially exposed by etching the alumina matrix to a desired depth. In the current study, MWCNT samples with  $\sim 40$ – $60$  nm protruded length were used. The diameters of these MWCNT range from 30 to 40 nm with  $\sim 40$ – $50$  nm interchannel separation. As shown in Fig. 1(a), the VAMWCNT form a two-dimensional (2D) hexagonal close-packed superlattice according to the underlying channel patterns of the porous alumina template. This superlattice has a lattice constant of

$\sim 100$  nm, which is about a few hundred times larger than the normal atomic crystal lattice constant. Since atomic lattices can be resolved by an AFM probe with a tip radius of tens of nanometers, we employed a colloidal probe with a tip radius of 15  $\mu\text{m}$  to investigate the friction behavior of this VAMWCNT superlattice. Borosilicate glass microspheres (Duke Scientific Corporation, diameter of  $14.5 \pm 1.0$   $\mu\text{m}$ ) were attached to regular AFM cantilevers using Devcon 5-Minute® Epoxy adhesive. The scan size was 1  $\mu\text{m}$  with a scan speed of 2000 nm/s. The tip profile of both the regular AFM tip and the colloidal AFM probe were characterized by using a TGG01 (MicroMasch) calibration grating with well distributed arrays of sharp tips.

As shown in Fig. 1(b), a typical scan trace in both forward (left to right) and backward directions at a constant normal load by using a colloidal AFM probe forms a friction “loop.” The sawtooth modulation resembled the periodicity of the VAMWCNT superlattice as described earlier. This is analogous to the atomic stick-slip pattern that repeats once every atomic spacing. As a result, the corresponding lateral force microscopy (LFM) image clearly characterized the periodic arrangements of carbon nanotube superlattices.<sup>15</sup> However, a very different reverse stick-slip behavior was clearly observed upon closer inspection [Fig. 1(b)], where the stick is abrupt and the slip is gradual. This is in sharp contrast with the regular gradual-stick-rapid-slip motion observed in other LFM studies of frictions at atomic scales. The mechanics of atomic stick-slip behavior was explained by Tománek *et al.*<sup>17</sup> based on the Tomlinson model to be associated with gradual elastic energy building up in the AFM cantilever and at the contact, and then the sudden release of such energy when it surpasses the periodic interfacial potential energy barrier defined by the atomic structure of the surface and the contact. It is worth noting that in many atomic scale LFM studies that adopted this interpretation, the sample surfaces were assumed to be atomically flat (crystalline samples were cleaved in high vacuum), i.e., no surface topology effect considered.

Further inspection of the surface profile of the colloidal AFM probe using the TGG01 calibration grating revealed nanoscale asperities on the seemingly smooth glass sphere surface [Fig. 1(c)]. Since the sizes of the asperities are about the same size as a regular AFM tip with a tip radius of

<sup>a)</sup>Electronic mail: jlou@rice.edu.

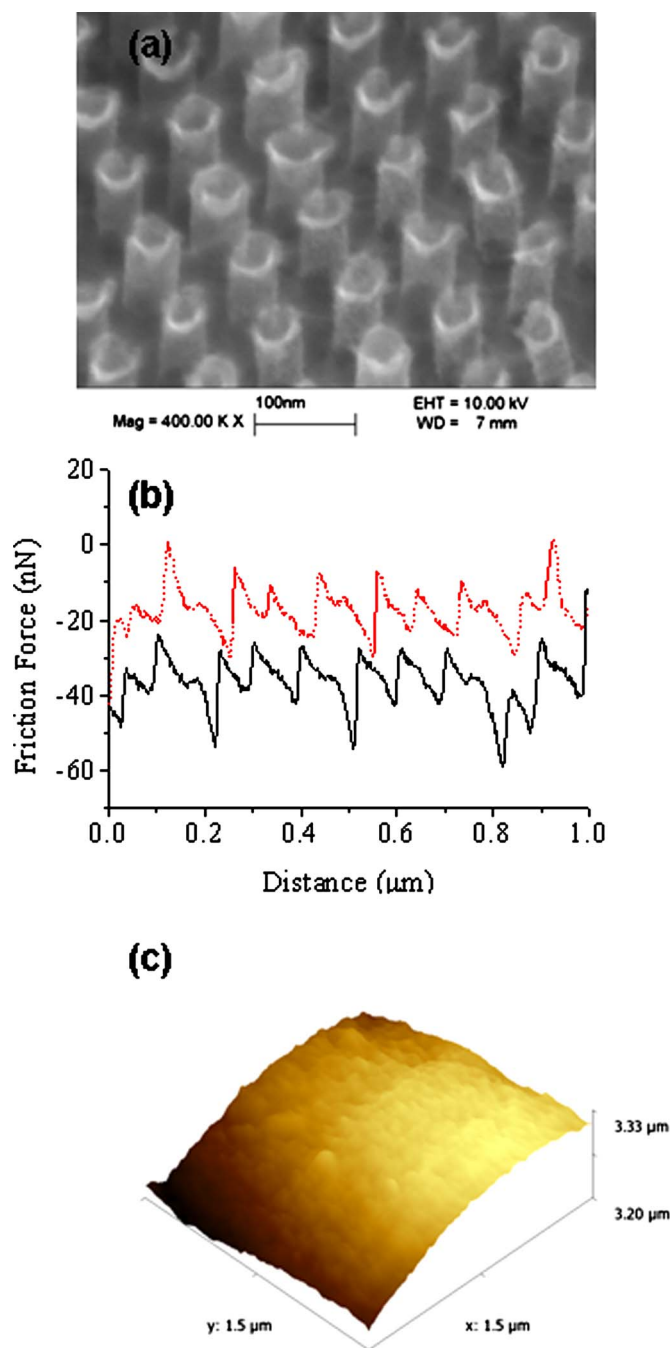


FIG. 1. (Color online) (a) SEM images of the VAMWCNT superlattice. (b) Reverse stick-slip behavior of VAMWCNT superlattices of 30 nm protruded length scanned with a colloidal AFM probe. (c) Three-dimensional profile of the colloidal AFM probe.

$\sim 10\text{--}50$  nm, the friction experiments on VAMWCNT superlattices were repeated using a regular AFM tip and the same reverse stick-slip behavior was again observed [Fig. 2(c)]. Recall that since the separation between the vertically aligned MWCNTs is  $\sim 40\text{--}60$  nm, it is very likely that the tip might slide down the valley in between nanotubes and feel the surface topology during scanning. This scenario is very different from previous tribological studies of closely packed CNT bundles.<sup>13</sup> Thin-walled MWCNTs are flexible and may easily buckle.<sup>12,14</sup> It was estimated that the critical shell buckling load for MWCNT with similar dimensions was  $2\text{--}2.5$   $\mu\text{N}$  and the maximum compressive force on individual MWCNT was computed to be  $\sim 2$   $\mu\text{N}$  even when

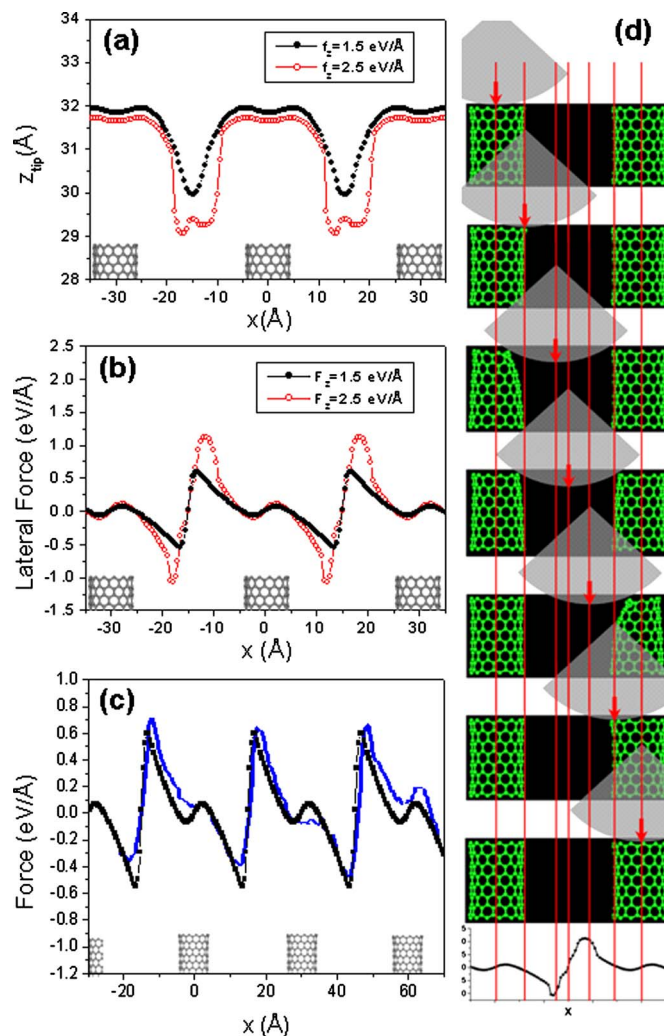


FIG. 2. (Color online) Interaction between the tip and CNT arrays obtained from MD simulation. (a) Vertical displacement of the tip and (b) lateral force experienced by the tip vs the sliding distance along the CNT arrays with normal force 1.5 and 2.5 eV/Å. (c) Reverse stick-slip behavior of VAMWCNT superlattices scanned with a regular AFM tip compared to the simulated lateral force vs sliding distance curve (after appropriate scaling). (Black square: simulated data; blue line: experimental data). (d) Detailed sliding process of the tip along the CNT arrays [(a)–(g)] and the corresponding lateral force on the cantilever (h) by MD simulation. For clarity, only part of the tip that is interacting with CNT arrays is shown.

the normal load applied by AFM tip was approaching zero.<sup>14</sup> In other words, VAMWCNT arrays would experience shell buckling events throughout the LFM experiments. This elastic instability combined with surface topology effects were thought to be responsible for the rapid stick and subsequent gradual slip of the AFM tip over MWCNTs with comparable dimension [Fig. 2(d)].

Due to the lack of direct experimental observation of the tip/VAMWCNT superlattice interface, molecular dynamics (MD) simulations were performed in order to shed light on this interesting and important behavior. In order to mimic the experimental condition which could capture the essential physics, a one-dimensional single-walled CNT array was used to represent the 2D MWCNT superlattice in our simulation. Short (13,0) single walled nanotubes (diameter  $\sim 0.94$  nm, height  $\sim 1.5$  nm, and aspect ratio  $\sim 1.6$  which is close to the real samples) were placed along the  $x$  axis (as shown in Fig. 2) with a tube-tube spacing of 3 nm. AFM tip was modeled as a rigid sphere with a diameter of 4 nm. In

order to further simplify the problem, the interaction between the tip and the carbon atoms are described by the repulsive part of the simple Leonard–Jones potential:  $V(d)=4\varepsilon(\sigma/d)^{12}$ ,<sup>12</sup> where  $\varepsilon=0.1$  eV/Å,  $\sigma=0.3$  nm, and  $d$  is the distance between the tip surface and the carbon atom. The effects of surface topology on tip vertical displacement and lateral force as a function of normal load were shown in Figs. 2(a) and 2(b), respectively. More importantly, the simulated scanning process of the tip over CNT arrays clearly demonstrated the reverse quick-stick-gradual slip behavior observed in the experiments along with the unambiguous evidence of CNT shell buckling [Fig. 2(d)]. This is further confirmed in Fig. 2(c) by the close qualitative match of the key features of the curves for the experimental and simulated lateral force as a function of sliding distance. Simulation results reveal that the penetration of the tip into the valley between the nanotubes [Fig. 2(a)] plays a critical role in the reverse stick-slip behavior. The penetrated tip interacts strongly with the tubes on both sides and thus, changes the lateral force from its minimum to a maximum in a very short distance resulting rapid sticking. In contrast, the gradual slipping occurs over much longer distance ( $\sim 80\%$ – $90\%$  of the superlattice constant) because it includes both the sliding on the top of the tube and release of energy on both sides of the graphitic wall [Fig. 2(d)]. Due to the hollow tube structure, a local minimum emerges in the lateral force curve when the tip passes the center of the tube. As shown in Figs. 1(b) and 2(c), this property was observed in the experimental stick-slip lines, which is a strong support to the validity of the theoretical simulation.

In summary, AFM based nanofriction experiments were performed on VAMWCNT arrays and a reverse stick-slip behavior was observed in this system for the first time. MD

simulations reveal that this is induced by the combined effects of sample surface topology and elastic shell buckling of CNT.

J.L. would like to acknowledge Professor K.-S. Kim and Q. Li of Brown University for useful discussions. The authors gratefully acknowledge the support from the Center for Biological and Environmental Nanotechnology (NSF Award No. EEC-0647452). This material is also based on research sponsored by the Air Force Research Laboratory under Agreement No. FA8650-07-2-5061.

- <sup>1</sup>M. R. Falvo, G. J. Clary, R. M. Taylor, V. Chi, F. P. Brooks, Jr., S. Washburn, and S. Superfine, *Nature (London)* **389**, 582 (1997).
- <sup>2</sup>M. P. de Boer and T. M. Mayer, *MRS Bull.* **26**, 302 (2001).
- <sup>3</sup>R. W. Carpick, *Science* **313**, 184 (2006).
- <sup>4</sup>A. Socoliuc, E. Gencco, S. Maier, O. Pfeiffer, A. Baratoff, R. Bennewitz, and E. Meyer, *Science* **313**, 207 (2006).
- <sup>5</sup>C. M. Mate, G. M. McClelland, R. Erlandsson, and S. Chiang, *Phys. Rev. Lett.* **59**, 1942 (1987).
- <sup>6</sup>R. W. Carpick and M. Salmeron, *Chem. Rev. (Washington, D.C.)* **97**, 1163 (1997).
- <sup>7</sup>S. Morita, S. Fujisawa, and Y. Sugawara, *Surf. Sci. Rep.* **23**, 3 (1996).
- <sup>8</sup>K. L. Johnson and J. Woodhouse, *Tribol. Lett.* **5**, 155 (1998).
- <sup>9</sup>A. Socoliuc, R. Bennewitz, E. Gnecco, and E. Meyer, *Phys. Rev. Lett.* **92**, 134301 (2004).
- <sup>10</sup>B. Ni and S. B. Sinnott, *Surf. Sci.* **487**, 87 (2001).
- <sup>11</sup>H. Kinoshita, I. Kume, M. Tagawa, and N. Ohmae, *Appl. Phys. Lett.* **85**, 2780 (2004).
- <sup>12</sup>K. Miyake, M. Kusunoki, H. Usami, N. Umehara, and S. Sasaki, *Nano Lett.* **7**, 3285 (2007).
- <sup>13</sup>P. L. Dickrell, S. B. Sinnott, D. W. Hahn, N. R. Ravivkar, L. S. Schadler, P. M. Ajayan, and W. G. Sawyer, *Tribol. Lett.* **18**, 59 (2005).
- <sup>14</sup>Z. H. Xia, J. Lou, and W. A. Curtin, *Scr. Mater.* **58**, 223 (2008).
- <sup>15</sup>J. Lou and K.-S. Kim, *Mater. Sci. Eng., A* **483-484**, 664 (2008).
- <sup>16</sup>J. Li, C. Papadopoulos, and J. M. Xu, *Appl. Phys. Lett.* **75**, 367 (1999).
- <sup>17</sup>D. Tománek, W. Zhong, and H. Thomas, *Europhys. Lett.* **15**, 887 (1991).